leating of Laser Mirrors,

lastic Wave Propagation,

:h., vol. 3, 46, pp. 539–

Received June 27, 1988

AN EIGENFUNCTION APPROACH TO SINGULAR THERMAL STRESSES IN BONDED STRIPS

James P. Blanchard
Department of Nuclear Engineering and Engineering Physics
University of Wisconsin–Madison
Madison, Wisconsin 53706

Nasr M. Ghoniem
Boelter Hall
University of California, Los Angeles
Los Angeles, California 90024

Solutions for thermal stress singularities in finite bonded strips are sought by using an eigenfunction expansion in the neighborhood of the singularity. The coefficients in the resulting series are determined by satisfying the boundary conditions on surfaces far removed from the singularity either pointwise or in an integrated sense. The latter of these techniques is found to be more reliable. The accuracy of the solution is checked by comparing it to a semianalytical solution for thermal stresses in bonded quarter planes, which is derived by using the Mellin transformation. It is shown that the eigenfunction approach provides accurate solutions for the leading term in the series, thus capturing the essence of the thermal stress fields near the edge of the interface. The far-field solutions, however, are found to feature excessive inaccuracies, which are attributed to numerical errors.

INTRODUCTION

Bonded joints are of interest in many engineering disciplines, including electronics, aerospace, and fusion energy. Because of surface and bulk heating associated with the fabrication and operation of such components, thermal stresses are nearly always encountered, so efforts to understand the details of the resultant fields is important. A common technique for the analysis of bonded structures utilizes variational principles to minimize the complementary potential energy of the structure, based on some assumed displacement profile. This work began with Weitsmann [1], who included an adhesive layer between the two primary layers. The displacements were assumed to be quadratic and/or cubic polynomials, and the shear and normal stresses were found to peak at the interface edge. Similar work has been conducted by Chen,

This research was performed under appointment to the Magnetic Fusion Energy Technology Fellowship Program administered at Oak Ridge Associated Universities for the United States Department of Energy. The financial support of the Office of Fusion Energy, U.S. Department of Energy (grant DE-FG03-86ER52126), for Ghoniem is also appreciated.

Cheng, and Gerhardt [2], and H. E. Williams [3]. Williams considered thin layers by using matched asymptotic expansions for the displacement fields, giving a boundary layer with a width of the order of $\sqrt{t/l}$ (where t/l is the thickness-to-length ratio of the model) at the interface edge. These variational methods require a great deal of algebra for even the simplest geometries and offer little advantage over numerical results from commercial finite-element codes, which are also based on potential minimization and can analyze many geometries and loadings. Unfortunately, neither of these two methods has treated the edge singularities predicted by infinitesimal elasticity.

Many authors have studied stress singularities in bonded structures. Williams [4] studied stresses at the base of a crack by using an assumed solution for the stress function that is of the form (using the notation adopted for this paper) $\Phi(r, \theta; s) = r^{-s}F(\theta; s)$. This led to a solution that consisted of an expansion in terms of the eigenfunctions of the problem. Square root singularities were found in the stress fields at the tip of the crack. Applying a related technique to duplex models, Bogy [5,6] used the Mellin transformation to calculate the asymptotic solutions for stresses near the edge of the interface. He considered a model consisting of two perfectly bonded quarter planes, and the singularity was found to be material dependent (as opposed to the simple geometry dependence associated with typical crack singularities), and, in most cases, of the order of $r^{-\delta}$, where δ lies between 0 and 0.40. For certain other material parameter combinations, though, the singularity was shown to be either logarithmic or nonexistent. Wang and Choi [7] have made a similar study of crack-free singularities in anisotropic materials. Whereas Bogy only considered half spaces, Wang and Choi studied singularities in finite bodies by using boundary collocation techniques. This work follows earlier work by Fadle [8], who considered double eigenfunction expansions for the analysis of rectangular bodies. One set of the coefficients in the expansion was found by minimizing the errors on the boundary in the least square sense.

In addition to these analytical and semianalytical methods, a number of analyses have been conducted by using standard finite elements. The reliability of these methods has been studied by Bauld and Goree [9] and Whitcomb and Raju [10]. Bauld and Goree compared finite-element and finite-difference methods and concluded that the finite-difference method is superior because it "characterizes the stress distributions near an interface corner in a more realistic manner." Whitcomb and Raju reviewed the use of finite-element methods for analysis of bonded structures and found that standard finite elements are accurate to within two or three elements of the edge of the interface, regardless of the element size, indicating that these methods are useful for global solutions, but they do not accurately predict the near-edge fields. Hence, special elements must be used.

Finally, there are numerous studies of stress singularities in composite structures/materials, typified by the work of Pagano and Soni [11]. These structures feature many very thin layers of orthotropic materials, generally built up from fibers embedded in a resin matrix. Techniques for analyzing such structures are not generally applicable in the case of relatively few thick layers, because of the approximations needed to handle the complex material constitutive equations, the numerous layers generally used in such designs, and the very small thickness of the layers. However, the local fields are quite similar.

In this paper, singular thermal stress fields in finite bonded structures are sought with the use of eigenfunctions that satisfy the interface and near-edge boundary conditions. These functions are then combined with a particular solution for uniform thermal fields to obtain a composite solution in the form of an infinite series with unknown coefficients. The coefficients are then determined by satisfying an integral form of the far-field boundary conditions both pointwise and in a least squares sense. The objective of this paper is to show the applicability of these techniques to the determination of singular stress fields in finite bonded strips. Thus, the results should be useful in developing failure criteria in the vicinity of the edge of a bonded structure under thermal loading.

PROBLEM DESCRIPTION

The problem to be studied in this paper consists of two equal length, perfectly bonded strips that have different material properties, as shown in Fig. 1. The properties of the upper strip are denoted by a double prime (e.g., μ'', α''), while those of the lower strip are denoted by a single prime. The interface is assumed to be perfect, with no slipping, delamination, or cracking, and the strips are assumed to be in a state of plane stress or plane strain. Because the strips are assumed to be crack-free, the analysis presented here represents a study of the initiation of failure at the edge of the interface of a laminated structure. In bodies (either single- or multi-layered) containing cracks, linear elastic fracture mechanics predicts a stress field of the form

$$\sigma_{ij} \sim \frac{K}{r^{0.5+i\beta}} \qquad r \to 0 \tag{1}$$

at the tip of the crack, where r is the distance from the crack tip. (The imaginary part β of the order of the singularity is zero for single-material cracks.) The stress intensity factor K is considered to be a measure of the intensity of the stress singularity and has been shown experimentally to be a useful predictor of crack growth.

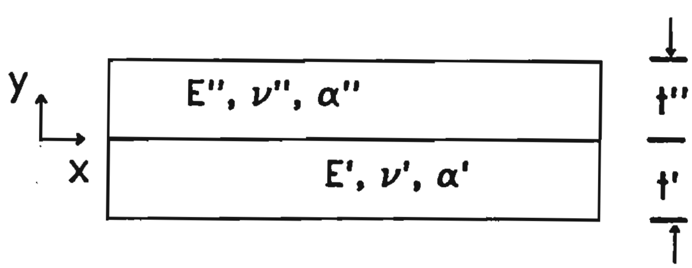

Fig. 1 Model used for analysis of singular stress fields in finite bodies.

As will be shown in the following section, the stress field in a crack-free, bonded structure is generally of the form

$$\sigma_{ij} \sim \frac{K}{r^{\delta}} \quad r \rightarrow 0 \tag{2}$$

where $0 \leq \delta \leq 0.41$. Therefore, crack-free, bonded components exhibit a relatively weak singularity analogous to that for the stress field near a crack tip. It is suggested that the initiation of failure in bonded structures can be predicted by the "stress intensity" associated with the edge of a perfect interface, making knowledge of the characteristics of such stress fields vital to the design of bonded structures. Therefore, characterization of the near-edge stress fields in crack-free structures is important. Experimental correlations will be necessary to establish relationships between edge delamination failure and the character of the near-edge stress fields in bonded strips.

GENERAL SINGULAR STRESS FIELDS

The stresses at the edge of the interface between two materials can be sought by considering bonded semi-infinite quarter planes [5]. The model used for this purpose is shown in Fig. 2. Using the Airy stress function, one can determine a stress field that satisfies the field equations in the bulk, the interface conditions, and the traction conditions on the free surfaces adjacent to the interface. This yields an infinite series with undetermined coefficients, which are to be determined by considering the finite extent of the original model shown in Fig. 1.

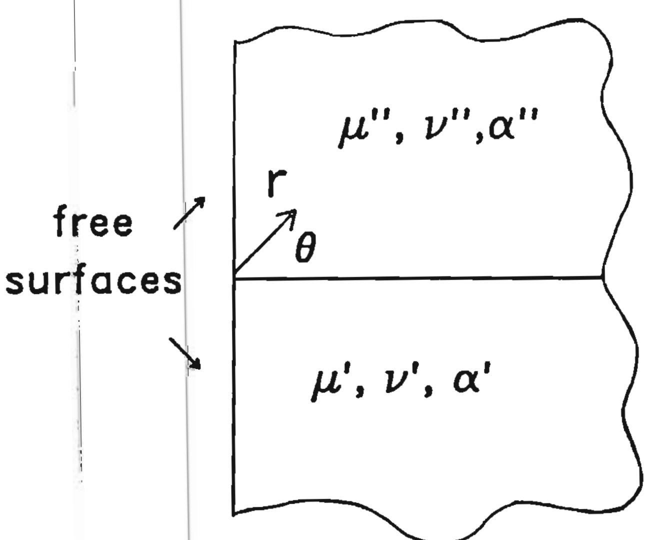

Fig. 2 Model for semi-infinite quarter planes to determine stresses at the edge of the interface.

The analysis begins with the two-dimensional, steady state, elastic field equations in polar coordinates (assuming no body forces are present), along with the traction-free boundary conditions and the assumed interface conditions:

Strain-displacement

$$\epsilon_{rr} = u_{r,r} \tag{3}$$

$$\epsilon_{\theta\theta} = \frac{u_r}{r} + \frac{u_{\theta,\theta}}{r} \tag{4}$$

$$\epsilon_{r\theta} = \frac{1}{2}\left(\frac{1}{r}u_{r,\theta} + u_{\theta,r} - \frac{u_\theta}{r}\right) \tag{5}$$

Stress-strain

$$\sigma_{rr} = 2\mu\epsilon_{rr} + \lambda\epsilon_{ll} - (2\mu + 3\lambda)\alpha T \tag{6}$$

$$\sigma_{\theta\theta} = 2\mu\epsilon_{\theta\theta} + \lambda\epsilon_{ll} - (2\mu + 3\lambda)\alpha T \tag{7}$$

$$\sigma_{r\theta} = 2\mu\epsilon_{r\theta} \tag{8}$$

Equilibrium

$$\sigma_{rr,r} + \frac{\sigma_{r\theta,\theta}}{r} + \frac{\sigma_{rr} - \sigma_{r\theta}}{r} = 0 \tag{9}$$

$$\frac{\sigma_{\theta\theta,\theta}}{r} + \sigma_{r\theta,r} + 2\frac{\sigma_{r\theta}}{r} = 0 \tag{10}$$

Boundary conditions: ($\theta = \pm\pi/2$)

$$\sigma_{\theta\theta} = \sigma_{r\theta} = 0 \tag{11}$$

Interface conditions: ($\theta = 0$)

$$\sigma'_{\theta\theta} = \sigma''_{\theta\theta} \tag{12}$$

$$\sigma'_{r\theta} = \sigma''_{r\theta} \tag{13}$$

$$u'_r = u''_r \tag{14}$$

$$u'_\theta = u''_\theta \tag{15}$$

In these equations, σ_{ij} represents a stress, ϵ_{ij} represents a strain, u_r and u_θ represent the radial and azimuthal deflections, respectively, and λ and μ are the Lamé material constants. Also, α is the thermal expansion coefficient, and T is the difference between the temperature in the component and some zero-stress reference temperature.

To reduce the problem to determination of a scalar function, the Airy stress function Φ is introduced according to the standard definition:

$$\sigma_{rr} = \frac{1}{r}\Phi_{,r} + \frac{1}{r^2}\Phi_{,\theta\theta} \tag{16}$$

$$\sigma_{\theta\theta} = \Phi_{,rr} \tag{17}$$

$$\sigma_{r\theta} = \frac{1}{r^2}\Phi_{,\theta} - \frac{1}{r}\Phi_{,r\theta} \tag{18}$$

Combining these equations with the strain-displacement and stress-strain equations, the displacements are found to be

$$u_{r,r} = \frac{1}{2\mu}\left[\frac{1}{r}\Phi_{,r} + \frac{1}{r^2}\Phi_{,\theta\theta} - \left(1 - \frac{m}{4}\right)\nabla^2\Phi\right] + n\alpha T \tag{19}$$

and

$$u_{\theta,r} - \frac{u_\theta}{r} + \frac{1}{r}u_{r,\theta} = \frac{1}{\mu}\left(\frac{1}{r^2}\Phi_{,\theta} - \frac{1}{r}\Phi_{,r\theta}\right) \tag{20}$$

where

$$m = \begin{cases} 4/(1+\nu) & \text{for plane stress} \\ 4(1-\nu) & \text{for plane strain} \end{cases} \tag{21}$$

and

$$n = \begin{cases} 1 & \text{for plane stress} \\ (1+\nu) & \text{for plane strain} \end{cases} \tag{22}$$

To satisfy the compatibility equation, the stress function must satisfy the following fourth-order partial differential equation (again assuming no body forces):

$$\nabla^4\Phi + qE\nabla^2\alpha T = 0 \tag{23}$$

where q is given by

$$q = \begin{cases} 1 & \text{for plane stress} \\ 1/(1-\nu) & \text{for plane strain} \end{cases} \tag{24}$$

Solving for the stress function, subject to the appropriate surface traction and interface conditions, provides a means for computing the steady state thermal stresses, strains, and displacements in a planar medium.

In this study, the thermal fields are harmonic (satisfying Fourier's Law of conduction for a body in steady state), so the stress function is governed by

$$\nabla^4 \Phi = 0 \tag{25}$$

To reduce this partial differential equation for the Airy stress function to an ordinary differential equation, the solution is assumed to be of the form

$$\Phi = r^{-s} F(\theta) \tag{26}$$

Under this transformation, the equation for the stress function (Eq. (25)) becomes

$$\left(\frac{d^2}{d\theta^2} + s^2\right)\left(\frac{d^2}{d\theta^2} + (s+2)^2\right) F = 0 \tag{27}$$

Also, the stresses are given by

$$\sigma_{rr} = \left(\frac{d^2}{d\theta^2} - s\right) F r^{-(s+2)} \tag{28}$$

$$\sigma_{\theta\theta} = s(s+1) F r^{-(s+2)} \tag{29}$$

and

$$\sigma_{r\theta} = (s+1) \frac{dF}{d\theta} r^{-(s+2)} \tag{30}$$

For $s \neq 0, -2$, the general form of the stress function is

$$F = a \sin s\theta + b \cos s\theta + c \sin (s+2)\theta + d \cos (s+2)\theta \tag{31}$$

where a, b, c, and d are unknown constants.

Given a solution for the stress function in each quarter plane of the model, the full solution is obtained by using the boundary and interface conditions to determine the four unknown constants in each strip. This process is begun by rewriting the stresses and displacements in terms of the unknown constants a, b, c, and d. Inserting Eq. (31) into Eqs. (28–30), one obtains the following equations for the stresses:

$$\sigma_{rr} = [-as \sin s\theta - bs \cos s\theta - c(s+4) \sin (s+2)\theta$$

$$- d(s+4) \cos (s+2)\theta](s+1) r^{-(s+2)}$$

$$\sigma_{\theta\theta} = [a \sin s\theta + b \cos s\theta + c \sin (s+2)\theta + d \cos (s+2)\theta] s(s+1) r^{-(s+2)}$$
$$\sigma_{r\theta} = [as \cos s\theta - bs \sin s\theta + c(s+2) \cos (s+2)\theta - d(s+2) \sin (s+2)\theta](s+1) r^{-(s+2)} \tag{32}$$

The displacements can be found by inserting the solution for F into Eqs. (19) and (20), and integrating them. First, though, one requires knowledge of the thermal field, which is assumed to be constant. This thermal field yields the following displacement fields:

$$u_r = u_0 \cos \theta + v_0 \sin \theta + n\alpha T_0 r + \frac{r^{-(s+1)}}{2\mu} [sa \sin s\theta + sb \cos s\theta + (s+m)c \sin (s+2)\theta + (s+m)d \cos (s+2)\theta]$$
$$u_\theta = -u_0 \sin \theta + v_0 \cos \theta + w_0 r - \frac{r^{-(s+1)}}{2\mu} [sa \cos s\theta - sb \sin s\theta + (s+2-m)c \cos (s+2)\theta + (s+2-m)d \sin (s+2)\theta] \tag{33}$$

where u_0 and v_0 represent rigid body displacements in the x and y directions, respectively, and w_0 represents a rigid body rotation.

By using these equations for the stresses and displacements, the boundary and interface conditions can be used to determine the eight unknown constants.

Application of the boundary and interface conditions provides the following system of eight equations for the unknown constants:

$$\begin{aligned}
-a' \sin \xi + b' \cos \xi + c' \sin \xi - d' \cos \xi &= 0 \\
a'' \sin \xi + b'' \cos \xi - c'' \sin \xi - d'' \cos \xi &= 0 \\
a's \cos \xi + b's \sin \xi - c'(s+2) \cos \xi - d'(s+2) \sin \xi &= 0 \\
a''s \cos \xi - b''s \sin \xi - c''(s+2) \cos \xi + d''(s+2) \sin \xi &= 0 \\
b' + d' - b'' - d'' &= 0 \\
sa' + (s+2)c' - sa'' - (s+2)c'' &= 0 \\
sb' + (s+m')d' - ksb'' - k(s+m'')d'' &= L_1 \\
-sa' - (s+2-m')c' + ksa'' + k(s+2-m'')c'' &= 0
\end{aligned} \tag{34}$$

where

HOMOGENEOUS

The homogeneous so
zero. A nontrivial solu
implied by the above
of the form

where Δ is given by

and

and

The values of s corre
next section.

Because the strai
to $r^{-2(s+2)}$. Hence, for
Therefore, our interes
-1. In addition, root
fields, so they are of
nation of materials), s

A material-depen

determines the exister

where

$$k = \mu'/\mu''$$

$$\xi = s\pi/2 \tag{35}$$

$$L_1 = -2\mu'(n'\alpha'T_0' - n''\alpha''T_0'')r^{(s+2)}$$

HOMOGENEOUS SOLUTION

The homogeneous solution of the problem is found by setting the temperature to zero. A nontrivial solution to this equation exists only if the determinant of the matrix implied by the above 8 × 8 system is zero. This leads to a characteristic equation of the form

$$\Delta(s) = 0 \tag{36}$$

where Δ is given by

$$\Delta = [(k_1 - k_2)\cos^2(\xi) - k_1(s+1)^2]^2$$
$$+ k_3^2\cos^2(\xi)\sin^2(\xi) - k_2^2(s+1)^2 \tag{37}$$

and

$$k_1 = 2(k-1) \tag{38}$$

$$k_2 = km'' - m' \tag{39}$$

and

$$k_3 = km'' + m' \tag{40}$$

The values of s corresponding to the roots of the determinant are discussed in the next section.

Because the strain energy density is proportional to σ_{ij}^2, it will be proportional to $r^{-2(s+2)}$. Hence, for the total strain energy to be finite, s must be less than -1. Therefore, our interest lies in roots of the determinant that have real parts less than -1. In addition, roots that lie in the region $-2 < s < -1$ lead to singular stress fields, so they are of particular interest. For all k_1, k_2, and k_3 (i.e., for any combination of materials), $s = 0, -1$, and -2 are zeroes.

A material-dependent parameter P, defined as

$$P = k_2(2k_1 - k_2) \tag{41}$$

determines the existence of roots on the interval $-2 < s < -1$. As it turns out, this parameter is proportional to the derivative with respect to s of the determinant Δ at $s = -2$, so it is an indicator of the slope of the determinant at this point. For $P > 0$, there is exactly one zero on the interval $-2 < s < -1$, and it is a simple zero. For all admissible values of the material constants (i.e., $0 < \nu < \frac{1}{2}$), this zero occurs between -1.59 and -2.0. As P approaches zero, the zero of the determinant moves closer to $s = -2$ until, when $P = 0$, there are no zeroes on $-2 < s < -1$ and the zero at $s = -2$ becomes a double root. Finally, for $P > 0$, there are no zeroes on $-2 < s < -1$ and the zero at $s = -2$ is simple; also, there is a simple zero between -2.4 and -2.0.

As was mentioned previously, this paper will deal exclusively with material combinations that feature algebraic singularities at the edge of the interface (i.e., those for which $P = k_2(2k_1 - k_2) > 0$). For these material combinations, the root at $s = -1$ can be shown to represent the two rigid body translations, while the root at $s = -2$ represents a rigid body rotation. It is the other roots that contribute to the stress fields of interest.

In general, the only integer roots of the determinant are at $s = -2, -1$, and 0, but for certain material property combinations, there are other integer roots. If one assumes an integer solution, the determinant can be written

$$\Delta = \left\{\left[k_1(s+1)^2 - (k_1 - k_2)\cos^2\frac{s\pi}{2}\right]^2 - k_2^2(s+1)^2\right\} \tag{42}$$

If s is an odd integer (i.e., $s = -(2i-1)$, $i = 1, 2, 3, \ldots,$), then $\cos s\pi/2 = 0$ and the determinant can be written

$$\Delta = -4(i-1)^2 k_1^2\left[2(i-1) + \frac{k_2}{k_1}\right]\left[2(i-1) - \frac{k_2}{k_1}\right] \tag{43}$$

From this equation, one can see that there are odd integer roots of the determinant if k_2 is an even multiple of k_1.

If s is an even integer (i.e., $s = -2j$, $j = 1, 2, 3, \ldots,$), then $\cos s\pi/2 = \pm 1$ and the determinant can be written

$$\Delta = 4j(j-1)k_1^2\left[2(j-1) + \frac{k_2}{k_1}\right]\left[2j - \frac{k_2}{k_1}\right] \tag{44}$$

Again, there are additional integer roots when k_2 is an even multiple of k_1. As an example, consider the case where $k_2 = 8k_1$. Equation (43) indicates that there is a root for $i = 5$ ($s = -9$), while Eq. (44) indicates a root at $j = 4$ ($s = -8$). These eigenvalues must be accounted for when solutions for stresses in finite bodies are sought.

Besides the real roots on the interval $-2 < s < 0$, there are an infinite number of complex roots. A typical example of the spectrum of complex roots, determined numerically, is shown in Fig. 3. Several observations can be made regarding these complex roots:

1. They always appear as complex conjugates.
2. For large negative real part, the real part of one root is about one unit from its neighbors.
3. For increasing negative real part, the magnitude of the imaginary part increases much more slowly than the magnitude of the real part.

These complex roots, combined with the real root on the interval $-2 < s < -1$ (if one exists), lead to a solution for the stresses and displacements in the form of an infinite series.

Because the problem being considered in this section is homogeneous, a nontrivial solution exists only when the determinant of the matrix represented by Eq. (34) vanishes. Therefore, the solution for the eight unknown constants cannot be fully determined. Only seven of the constants can be determined in terms of the eighth (in this paper a' will be taken to be the undetermined constant), so the following ratios are defined:

$$A' = 1 \qquad B' = \frac{b'}{a'} \qquad C' = \frac{c'}{sa'} \qquad D' = \frac{d'}{sa'} \tag{45}$$

and

$$A'' = \frac{a''}{a'} \qquad B'' = \frac{b''}{a'} \qquad C'' = \frac{c''}{sa'} \qquad D'' = \frac{d''}{sa'} \tag{46}$$

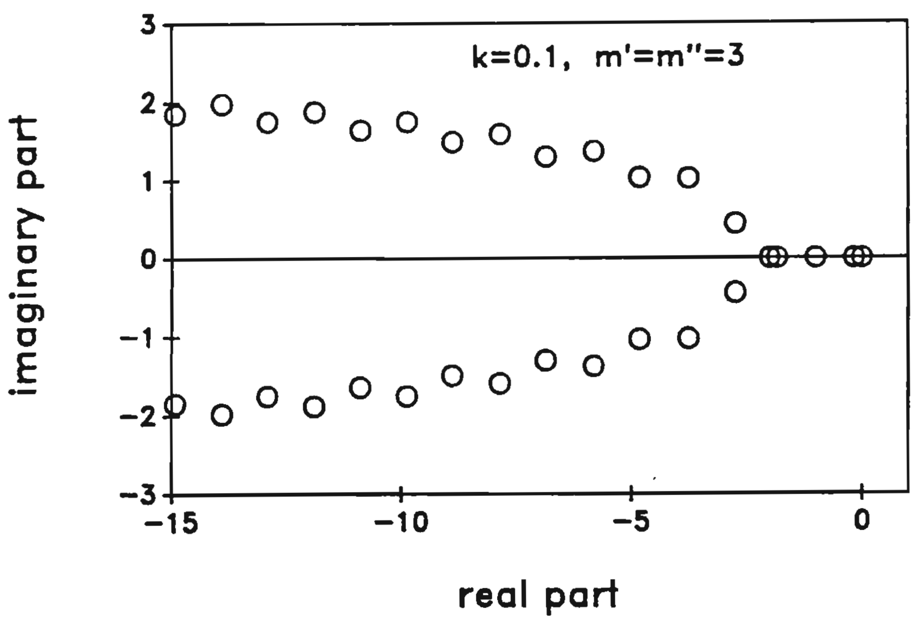

Fig. 3 Roots of determinant for $-15 \le s \le 0$. The number of roots is doubly infinite and the roots are symmetric about $\mathrm{Re}(s) = -1$.

Solving the system in Eq. (34) for these seven constants, one finds

$$
\begin{aligned}
B' &= \{k_1 s\eta[2s(s+1)+\gamma] + k_2 s\eta\delta - k_3\eta\gamma(s+2)\}/h \\
C' &= \{-k_1\gamma[2s(s+1)+\gamma] - k_2\gamma\delta - k_3\eta^2\}/h \\
D' &= \{-k_1\eta[2s(s+1)+\gamma] - k_2\eta\delta - k_3\eta\delta\}/h \\
A'' &= \{-k_1 s\delta[2s(s+1)+\gamma] - k_2 s\delta^2 - k_3(s+2)\eta^2\}/h \qquad (47)\\
B'' &= \{-k_2 s\eta[2s(s+1)+\gamma] - k_2 s\eta\delta - k_3\eta\gamma(s+2)\}/h \\
C'' &= \{-k_1\gamma[2s(s+1)+\gamma] - k_2\gamma\delta + k_3\eta^2\}/h \\
D'' &= \{k_1\eta[2s(s+1)+\gamma] + k_2\eta\delta - k_3\eta\delta\}/h
\end{aligned}
$$

where

$$h = -k_1 s\delta[2s(s+1)+\gamma] - k_2 s\delta^2 + k_3(s+2)\eta^2 \qquad (48)$$

$$\eta = -2\sin\xi\cos\xi \qquad (49)$$

$$\gamma = 2[(s+1) - \cos^2\xi] \qquad (50)$$

$$\delta = 2[(s+1) + \cos^2\xi] \qquad (51)$$

The quantity h is proportional to the second derivative of the determinant Δ, so it is only zero when the determinant has a double root. This case will not be dealt with in this paper, so one can proceed assuming $h \neq 0$.

Now that seven of the constants are known in terms of the eighth, the stresses and displacements can be expressed in terms of the unknown coefficients a_k, where the subscript k represents the k^{th} eigenvalue:

$$\sigma_{ij} = \sum_{k=1}^{\infty} a_k f_{ij(k)} r^{-(s_k+2)} \qquad (52)$$

$$u_r = \frac{1}{2\mu}\sum_{k=1}^{\infty} k_k f_{u_r(k)} r^{-(s_k+1)} \qquad (53)$$

$$u_\theta = \frac{1}{2\mu}\sum_{k=1}^{\infty} a_k f_{u_\theta(k)} r^{-(s_k+1)} \qquad (54)$$

where

$$f_{rr(k)} = [-A \sin s_k\theta - B \cos s_k\theta - (s_k + 4)C \sin (s_k + 2)\theta$$

$$- (s_k + 4)D \cos (s_k + 2)\theta]s_k(s_k + 1)$$

$$f_{r\theta(k)} = [A \cos s_k\theta - B \sin s_k\theta + (s_k + 2)C \cos (s_k + 2)\theta$$

$$- (s_k + 2)D \sin (s_k + 2)\theta]s_k(s_k + 1)$$

$$f_{\theta\theta(k)} = [A \sin s_k\theta + B \cos s_k\theta + s_kC \sin (s_k + 2)\theta \tag{55}$$

$$+ s_kD \cos (s_k + 2)\theta]s_k(s_k + 1)$$

$$f_{u_r(k)} = [A \sin s_k\theta + B \cos s_k\theta + (s_k + m)C \sin (s_k + 2)\theta$$

$$+ (s_k + m)D \cos (s_k + 2)\theta]s_k$$

$$f_{u_\theta(k)} = [A \cos s_k\theta - B \sin s_k\theta + (s_k + 2 - m)C \cos (s_k + 2)\theta$$

$$+ (s_k + 2 - m)D \sin (s_k + 2)\theta]s_k$$

Because the complex roots s_k appear as complex conjugates, the stresses and displacements in this series are real. It remains to determine the unknown series coefficients for a particular thermal field.

PARTICULAR SOLUTION FOR A UNIFORM TEMPERATURE CHANGE

For a uniform temperature change and for $2k_1 - k_2 \neq 0$, the particular solution is

$$a' = a'' = c' = c'' = 0 \tag{56}$$

and

$$b' = b'' = d' = d'' = \frac{2\mu'(n''\alpha''T_0'' - n'\alpha'T_0')}{2k_1 - k_2} \tag{57}$$

By using these constants, the stresses and displacements are found to be

$$\sigma_{xx} = 0$$

$$\sigma_{yy} = \frac{8\mu'(n''\alpha''T_0'' - n'\alpha'T_0')}{2k_1 - k_2}$$

$$\sigma_{xy} = 0 \tag{58}$$

$$u_x = \left[\frac{n''\alpha''T_0'' - n'\alpha'T_0'}{2k_1 - k_2}(m' - 4) + n'\alpha'T_0' \right] x$$

$$u_y = \left[\frac{n''\alpha''T_0'' - n'\alpha'T_0'}{2k_1 - k_2} m' + n'\alpha'T_0' \right] y$$

This particular solution consists of a uniform tension or compression (on the surfaces parallel to the interface) that is of sufficient magnitude to cause matching displacements in two strips that expand at different rates. This mechanism relies on the fact that two strips will generally experience different transverse displacements when they are loaded by equal tension or compression. Hence, the solution breaks down when the lateral displacements of the two strips are equal (i.e., when $2k_1 - k_2 = 0$).

This analysis leaves us with a solution of the form

$$\sigma_{rr} = \sum_{k=1}^{\infty} a_k f_{rr(k)} r^{-(s+2)} + 2b(1 - \cos 2\theta)$$

$$\sigma_{\theta\theta} = \sum_{k=1}^{\infty} a_k f_{\theta\theta(k)} r^{-(s+2)} + 2b(1 + \cos 2\theta)$$

$$\sigma_{r\theta} = \sum_{k=1}^{\infty} a_k f_{r\theta(k)} r^{-(s+2)} + 2b \sin 2\theta \tag{59}$$

$$u_r = \frac{1}{2\mu} \sum_{k=1}^{\infty} a_k f_{u_r(k)} r^{-(s+1)} + \frac{br}{2\mu}(m - 4\cos^2\theta) + n\alpha T_0 r$$

$$u_\theta = \frac{1}{2\mu} \sum_{k=1}^{\infty} a_k f_{u_\theta(k)} r^{-(s+1)} + \frac{2kbr}{2\mu} \sin 2\theta$$

where

$$b = \frac{2\mu'}{2k_1 - k_2}(n''\alpha T_0'' - n'\alpha T_0') \tag{60}$$

The rigid body motions have not been included in this equation, but they are important in the ensuing analysis of finite bodies. For any value of the series coefficients a_k, this general solution satisfies the equilibrium and compatibility equations in the interior of each of the two strips, the traction conditions on the free surfaces adjacent to the interface, and the interface conditions.

SOLUTIONS FOR FINITE BODIES

The series solution for the stresses and displacements near the edge of the interface between bonded structures satisfies the equilibrium and compatibility conditions in the interior of two bonded structures, and it satisfies the boundary conditions on the free surfaces adjacent to the interface, but it does not satisfy the remaining boundary conditions. Solutions for finite bodies must account for this deficiency. In this paper the model shown in Fig. 1 is used to explore the thermal stresses in bilayered structures. Because the thermal field and model geometry are symmetric about $x = l$, only half of the model must be considered, leaving only one singularity to accommodate. Since there is only one singularity, a single series solution, originating where the interface intersects the free surface, can be used to model the stresses throughout the body. The previously unknown coefficients must be determined such that the remaining boundary conditions are satisfied in some approximate manner. The additional stress boundary conditions are zero normal and shear stress on the surfaces parallel to the interface and zero shear stress along the symmetry line. The final boundary condition is that, along the symmetry line, the displacements in the axial (x) direction are uniform, which can be expressed by

$$\frac{\partial u_x}{\partial y} = 0, \text{ at } x = l \tag{61}$$

Putting this quantity into the series form used for the stresses and displacements, one finds

$$\frac{\partial u_x}{\partial y} = \frac{1}{2\mu} \sum_{k=1}^{\infty} a_k r^{-(s_k+2)} \left\{ -(s_k + 2) f_{u_r} \sin\theta \cos\theta + \frac{\partial f_{u_r}}{\partial \theta} \cos^2\theta + [(s_k + 2)\sin^2\theta - 1] f_{u_\theta} - \frac{\partial f_{u_\theta}}{\partial \theta} \sin\theta \cos\theta \right\} + \omega_0 \tag{62}$$

The following sections will focus on the various methods for determining the coefficients in the series to satisfy these additional boundary conditions.

POINT COLLOCATION

The first (and simplest) method for determining the unknown series coefficients is point collocation. This method determines the coefficients such that the boundary and symmetry conditions are satisfied exactly at discrete points, called collocation points. Because there are two boundary conditions at each point along the free surface or symmetry line, there must be two unknowns in the solution for each collocation point if the solution for the coefficients is to be uniquely determined. Hence, if m collocation points are used, the series solution must be truncated at $2m$ terms.

This is a drawback of the method, because it forces the use of more terms in the series as more collocation points are used to improve the resolution of the solution. One might anticipate that increasing the number of collocation points would always lead to a more accurate solution, but this is not necessarily the case. The magnitude of the n^{th} term in the series increases roughly as r^{n+1}, so it can be quite large on the boundary. Hence, the precision required for accurate analysis increases rapidly as more terms are used and, for a given computational precision, the accuracy of the solution will eventually decrease with increasing number of collocation points.

LEAST SQUARES COLLOCATION

An alternative method for determining the coefficients in the series is called, for lack of a better term, least squares collocation, following Wang and Choi [7]. This technique minimizes, in the least squares sense, the integral of the error in the boundary and symmetry conditions along the outside of the symmetric model. This process is begun by defining the following integral:

$$I = \int_{AB} (w_{yy}\sigma_{yy}^2 + w_{xy}\sigma_{xy}^2)dx + \int_{BC} \left(w_{xy}\sigma_{xy}^2 + \frac{\partial u_x^2}{\partial y} \right) dy + \int_{CD} (w_{yy}\sigma_{yy}^2 + w_{xy}\sigma_{xy}^2)dx \qquad (63)$$

which represents the integral of the errors in the series solution along the top, symmetry line, and bottom, respectively. This residual integrand is given by the square of the difference between the prescribed boundary conditions and boundary values calculated from the approximate series solution. In most thermal stress problems, the boundaries are traction-free, providing homogeneous boundary conditions. In this case the integrand is given by the stresses and displacements from the series solution alone. The normalization factors w_{ij} are used to nondimensionalize the stress terms in this integral, but they also can be adjusted to emphasize a particular boundary condition on a particular side in order to optimize the determination of the unknown series coefficients. For this study, these normalization coefficients were taken to be the inverse of the square of the shear modulus of the associated strip. For a given number of terms in the series solution, the minimization of this residual integral gives the best available solution for the unknown series coefficients. Inserting the series representations for the stresses and displacements into this integral, including the particular solution, and taking the partial derivative with respect to each coefficient yields the following system for the coefficients:

$$\mathbf{Ma} = \mathbf{q} \qquad (64)$$

where vector **a** is the vector of unknown coefficients and the matrix **M** and the vector **q** are given by

$$M_{ij} = \int_{AB} (w_{yy} f_{yy(i)} f_{yy(j)} + w_{xy} f_{xy(i)} f_{xy(j)}) dx$$

$$+ \int_{BC} \left(\frac{\partial u_{x(i)}}{\partial y} \frac{\partial u_{x(j)}}{\partial y} + w_{xy} f_{xy(i)} f_{xy(j)} \right) dy$$

$$+ \int_{CD} (w_{yy} f_{yy(i)} f_{yy(j)} + w_{xy} f_{xy(i)} f_{xy(j)}) dx$$

and

$$q_i = \int_{AB} w_{yy} \sigma_{yy}^{\text{part}} f_{yy(i)} dx + \int_{CD} w_{yy} \sigma_{yy}^{\text{part}} f_{yy(i)} dx \tag{65}$$

where

$$f_{yy} = \left[\frac{1}{2} (f_{rr} + f_{\theta\theta}) - \frac{1}{2} (f_{rr} - f_{\theta\theta}) \cos 2\theta + f_{r\theta} \sin 2\theta \right] r^{-(s+2)} \tag{66}$$

and

$$f_{xy} = \left[\frac{1}{2} (f_{rr} - f_{\theta\theta}) \sin 2\theta + f_{r\theta} \cos 2\theta \right] r^{-(s+2)} \tag{67}$$

For other loading conditions, only the definition of the forcing vector **q** changes. Because of the increase of the magnitude of each term in the series with increasing number of terms, the matrix in the above equation is ill-conditioned. In general, the matrix **M** has a condition number (as defined by Press et al. [12]) which is roughly double the size of the matrix, so the condition number is greater than 24 when only 12 terms in the series are used. This is greater than the precision of the floating point calculations on the computers used for this study, so one cannot expect substantial increases in accuracy when more than 12 terms are used.

COMPARISON OF POINT AND LEAST SQUARES COLLOCATION

For a given number of terms in the series solution for the stresses and displacements, the point collocation technique is much faster than the least squares method because

Table 1 Material properties used for comparison of solution methods for finite bodies

Material Properties	Top Layer	Bottom Layer
Elastic modulus (MPa)	20.69	6.89
Expansion coefficient (K^{-1})	13×10^{-6}	6.5×10^{-6}
Poisson's ratio	0.25	0.33
Thickness (cm)	5	5

it does not require integration. This is an important fact, but the accuracy of the two techniques must be compared before judgements can be made regarding the applicability of the two methods. The comparison between the two will be made using the material properties and dimensions used by Chen, Cheng, and Gerhardt [2], as given in Table 1. All comparisons will be made assuming plane stress conditions. For these properties, the first ten roots of the determinant are given in Table 2. The first root indicates a stress singularity of the order of 0.071, that is,

$$\sigma_{ij} \sim r^{-0.071} \quad r \rightarrow 0 \tag{68}$$

The point collocation analysis was conducted by using an equal number of collocation points on the four boundary segments for which the boundary conditions are not yet satisfied. Therefore, multiples of four collocation points were chosen, and multiples of eight terms in the series were necessary to satisfy the two conditions at each point. The residual integral in the least squares collocation approach is computed by using Gaussian quadrature (48 Gauss points).

The accuracy of the two collocation methods is checked in two ways:

1. By comparing the calculated stress fields along the boundary to the required boundary conditions. This is especialy important for the point collocation method,

Table 2 Roots of determinant for properties used in comparison of different solution methods

Real Part	Imaginary Part
− 1.9289152	0
− 2.8319658	0.3605005
− 3.8066561	0.8169434
− 4.8424640	0.9095635
− 5.8452727	1.1700548
− 6.8696655	1.1849641
− 7.8711809	1.3908065
− 8.8885541	1.3735112
− 9.8890007	1.5530388
−10.902214	1.5177934

because sat
limited erro
2. By checkir
number of
one exists)
technique i

Unfortunately,
the error in the
and least squar
difference betv
boundary cond
ticular solution
cases, the larg
conditions. As
with large osci
extent of these
scale to a poin
be visible. The
4, the error is

The poor
which shows
increasing nur
for two differe

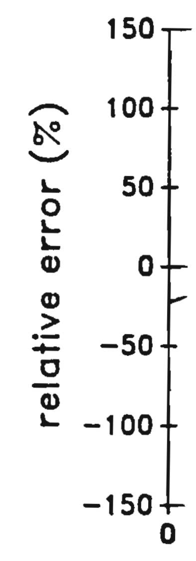

Fig. 4 Relative

:curacy of the two
garding the appli-
ill be made using
d Gerhardt [2], as
stress conditions.
·n in Table 2. The
is,

(68)

number of collo-
ary conditions are
were chosen, and
twc nditions at
app. .h is com-

wo ways:

ry to the required
:ollocation method,

because satisfying the boundary conditions exactly at discrete points allows unlimited errors elsewhere.

2. By checking the convergence of the coefficients in the series with increasing number of terms in the series. Because the coefficient of the singular term (if one exists) may be useful in design, its convergence is necessary if a particular technique is to be useful.

Unfortunately, the point collocation method does poorly on both tests. Fig. 4 shows the error in the normal stresses on the top surface, as calculated from both the point and least squares collocation methods. The errors shown in this figure are the relative difference between the stress computed by the approximation technique and the boundary condition, which is zero in this case. This error is normalized to the particular solution for the normal stress at the surface. The top surface exhibits, in both cases, the largest discrepancy between the calculated tractions and the traction-free conditions. As shown in the figure, the point collocation method yields surface stresses with large oscillations, giving errors that are many times the particular solution. The extent of these errors are not shown on the figure, because they would expand the scale to a point where the curves for the least squares collocation results would not be visible. The least squares collocation method fares much better. As shown in Fig. 4, the error is about 5–7% over most of the surface, and it peaks at about 27%.

The poor performance of the point collocation method is also shown by Fig. 5, which shows the convergence (or lack thereof) of the first series coefficient with increasing number of terms. While the least squares method converges quite well, for two different model lengths, the point collocation method shows almost no con-

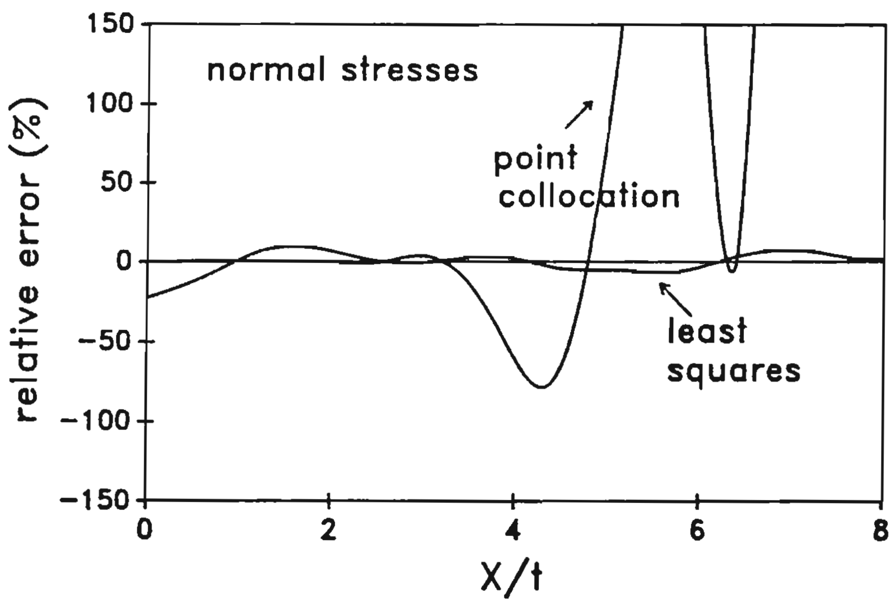

Fig. 4 Relative errors in normal stresses along top surface.

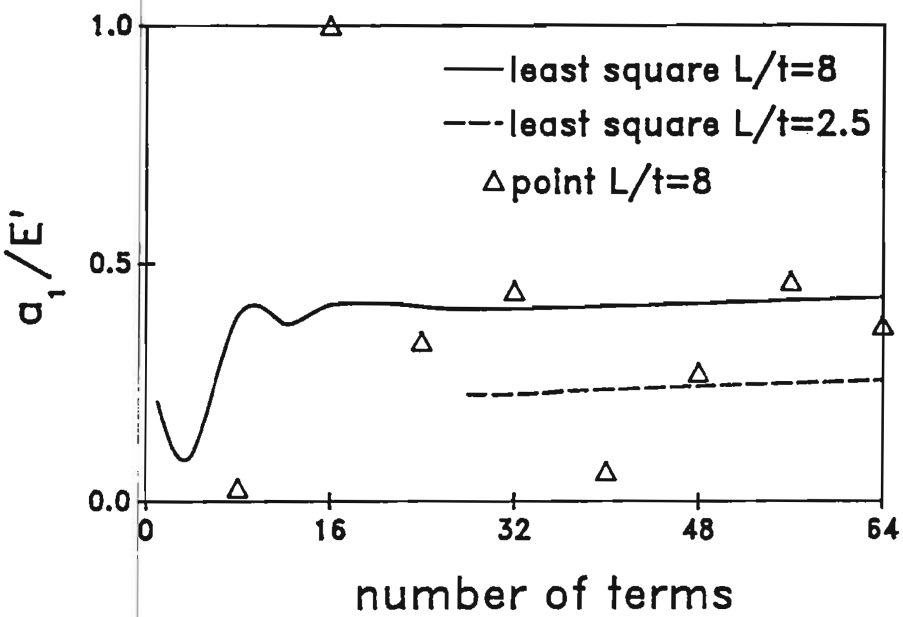

Fig. 5 Convergence of the first term in the series solution for increasing number of retained terms.

vergence. This latter point is somewhat disturbing, and it precludes further consideration of this technique. The point collocation method could, conceivably, be improved by fortuitous selecton of the collocation points, but this would detract from the versatility of the method. Hereinafter, only least squares collocation will be considered.

RESULTS FOR LEAST SQUARES COLLOCATION

As was mentioned in the previous section, the least squares collocation method shows promise as a useful technique because it exhibits good convergence of the stress series coefficients and it provides a reasonable characterization of the boundary conditions. This latter point is further exhibited in Fig. 6, which shows the relative error in both the shear and normal stresses along the top surface. This is essentially a magnified plot of the least squares collocation result for the normal stresses from Fig. 4, with the shear stresses shown as well. The error in the normal stress is on the order of 8% over most of the surface, with a peak of about 27% at $x = 0$, which represents the intersecton of the top surface with the free edge. This has been shown previously to be the point of maximum error in a similar study of composites [7]. The peak error in the shear stress is less than 10%. The relative errors on the other surfaces are lower than those on the top surface.

One difficulty with these collocation methods is the added precision required from the computation as more terms are used in the series solution for the stresses and displacements. Because the size of the terms increase roughly as r^{n+1}, for n

terms, the matrix is ill-conditioned, and high precision is needed for accurate solution of the system. This is shown in Figs. 7 and 8. The first figure shows the peak error in the normal stress on the top surface as a function of the number of terms in the series solution. The solid line represents the results of double precision calculations on a Cray-II computer (32-bit real number representations), while the circles show the results of double precision on a VAX 8200 (8-bit reals). The higher precision calculations show rapid decrease in the error until about 16 terms are used, then small improvement out to 64 terms. The lower precision calculations, on the other hand, show identical errors through about 27 terms, then a large error caused by the addition of just one term. A similar result is shown in Fig. 8, which plots the integral of the squares of the boundary conditions, as in Eq. 63, normalized by the integral of the particular solution. This figure also shows a marked increase in the error of the lower precision calculations past 27 terms. Clearly, high precision is required for the calculations.

A BENCHMARK PROBLEM

As was discussed, the least squares collocation method shows promise as a tool for studying singularities in bonded structures, but its utility is limited considering the errors on the boundary; the method is certainly not useful for calculating stresses in the bulk. The errors on the boundary come from a number of sources, including

1. Errors in the determination of the characteristic roots of the determinant, which becomes very important when large numbers of terms are used.

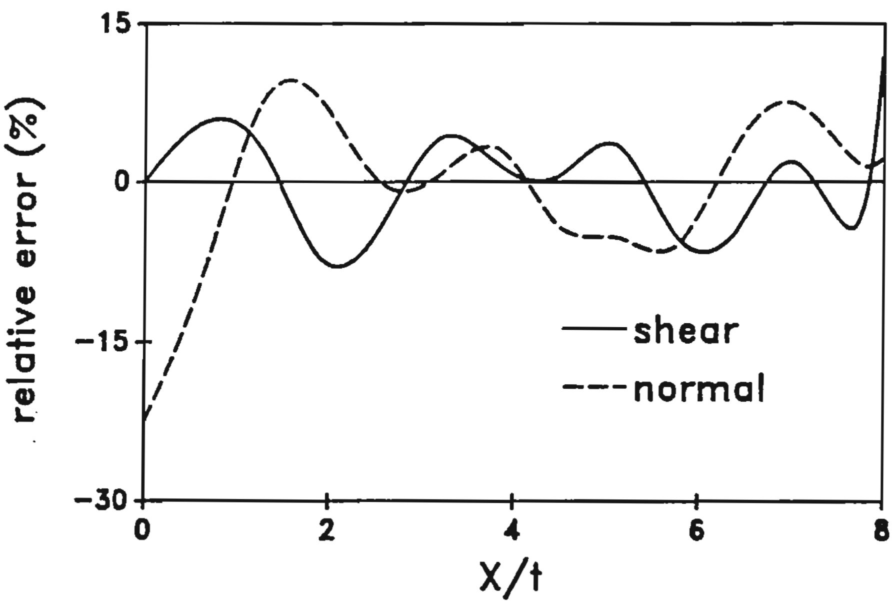

Fig. 6 Relative errors in shear and normal stresses along top surface for least squares collocation method.

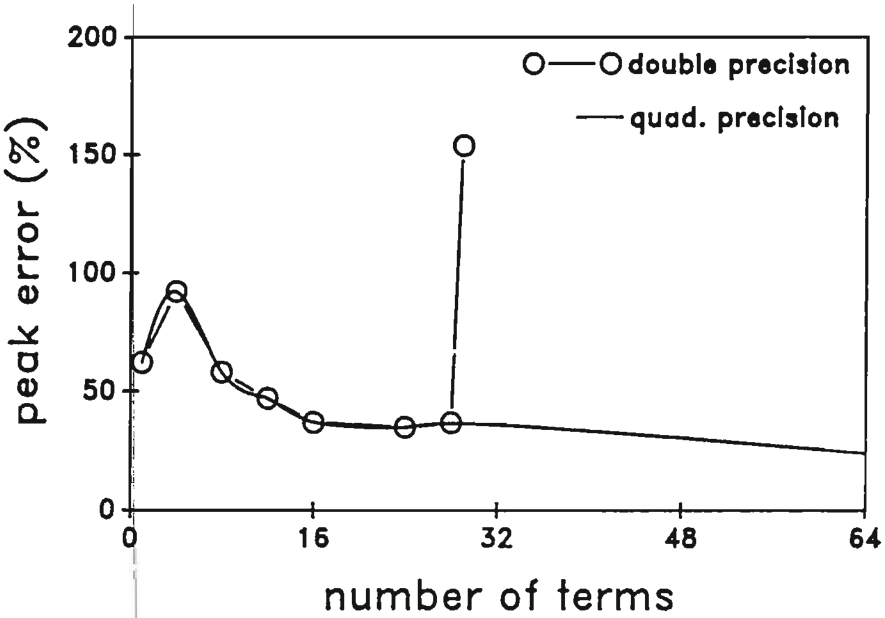

Fig. 7 Dependence of the peak error in the boundary conditions on the number of retained terms in the series for different amounts of precison in the numerical analysis.

2. Errors in solving the ill-conditioned linear system produced by the minimization of the integral around the boundary.
3. Errors in the quadrature.

Wang and Choi [7] used the same collocation technique to study crack-free singularities in anisotropic materials and obtained peak errors on the order of 1% on the boundary, as compared to the 27% in the calculations presented here. The difference, though, is that the anisotropic materials in Wang and Choi's study were identical, with the only difference between the two layers lying in the different fiber orientations. This case admits an infinite number of integer roots, in addition to an infinite number of complex roots much like those found in the case of dissimilar isotropic materials, so there is less error in determination of the eigenvalues (the integer eigenvalues are exact) and there are twice as many eigenvalues below a certain value. This last point is significant because the precision of a particular computer limits the allowable magnitude of the highest eigenvalue because the stresses are proportional to $r^{-(s+2)}$. Hence, the composite problem provides twice as many terms for a given precision.

The reduction of the integral of the tractions along the boundary with an increasing number of terms in the stress series, and the convergence of the first series coefficient, indicate that the calculations are reliable. This must be verified with a known solution.

Since the authors are not aware of any analyses of singularities in crackfree, finite, bonded structures composed of isotropic materials, an analytical solution must be used to verify the accuracy of the least squares collocation method. The benchmark problem chosen to show the usefulness of the least squares collocation method is one of thermal stresses in bonded quarter planes, which is analogous to the work of Bogy [6]. In order to benchmark a code for a rectangular, finite body, consider a half-space problem with a thermal field of the form

$$T = \begin{cases} T_0 & r < R_0 \\ 0 & r > R_0 \end{cases} \tag{69}$$

which represents a uniform temperature rise over a semicircle of radius R_0. The solution of the half-space problem gives the stresses and displacements throughout the bonded quarter planes. From this half space, one can extract a rectangle from within the semicircle of uniform temperature for analysis as a finite body. This finite body will have a uniform temperature change T_0 and surface tractions determined from the half-space solution. The least squares collocation method can then be used to solve for the boundary-layer stress intensity for this rectangle and compare it to the semianalytical solution found by using the Mellin transform.

Applying the Mellin transform to the field equations presented in the beginning of the previous section, and using the transformed boundary conditions, one arrives at the same system of equations, Eq. (34), as was found for the solution derived for use in the collocation solution. In this case, though, the solution of the system pro-

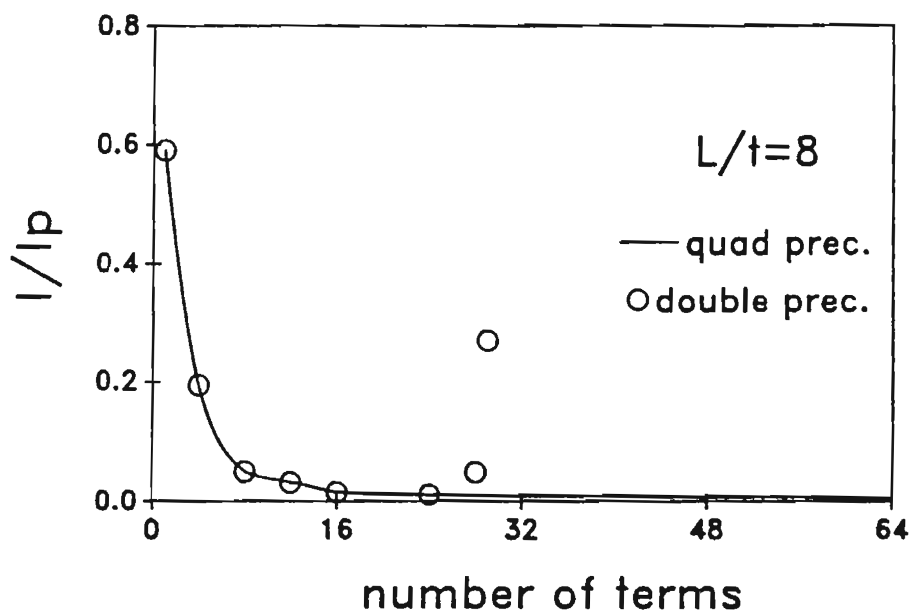

Fig. 8 Dependence of the error in the integral of the boundary and symmetry conditions on the number of retained terms in the series for different amounts of precision in the numerical analysis.

vides transformed stresses, which are given by equations of the form (using $\sigma_{\theta\theta}$ as an example):

$$\bar{\sigma}_{\theta\theta}(\theta = 0) = \frac{-(s+1)}{s\Delta}[Q_3 m' E' \alpha' \bar{T}' + Q_4 k m'' E'' \alpha'' \bar{T}''] \tag{70}$$

where

$$Q_3 = (1 - \cos y)[-(k-1)\delta(\gamma\delta - \eta^2) + k_3\eta^2 + k_2\gamma\delta] + \eta \sin y[-(k-1)(\gamma\delta - \eta^2) + 2km''\gamma] \tag{71}$$

and

$$Q_4 = (1 - \cos y)[(k-1)\delta(\gamma\delta - \eta^2) + k_3\eta^2 - k_2\gamma\delta] + \eta \sin y[(k-1)(\gamma\delta - \eta^2) + 2m'\gamma] \tag{72}$$

where $\bar{\sigma}$ represents the Mellin transform of σ. Inverting this relation gives the stresses in bonded elastic quarter planes. The Mellin inversion integral is given by

$$\sigma_{ij}(r, \theta) = \frac{1}{2\pi i}\int_{c-i\infty}^{c+i\infty} \bar{\sigma}_{ij}(s, \theta) r^{-(s+2)} ds \tag{73}$$

where c lies in a strip of regularity of the integrand. As was mentioned previously, we are concerned only with $s < -1$, so c lies between $\text{Re}(s) = -1$ and the first pole of the integrand associated with the inversion of the transformed stresses.

For plane stress the transformed thermal field is given by

$$\bar{T} = \frac{T_0 R_0^{s+2}}{s+2} \tag{74}$$

so, as seen from Eq. (70), there are poles in the transformed azimuthal stress at $s = 0, -2$ and at the roots of the determinant. According to the residue theorem, these poles provide the solution for thermal stress in bonded quarter-planes. Because the determinant in Eq. (70) is identical to the one derived previously, its roots are identical to those discussed earlier in this section. For the case studied here, all the poles are simple poles, but the one at $s = -2$ must be treated differently, using L'Hospital's rule.

At $s = -2$, the determinant has a double root, the transformed temperature has a simple pole, and Q_3 and Q_4 have simple roots, so the transformed stress has a simple pole. Using the residue theorem and L'Hospital's theorem, one finds that the residue at $s = -2$ provides

$$\sigma_{\theta\theta}(\theta = 0) = \frac{8\mu'(\alpha'' - \alpha')T_0}{2k_1 - k_2} \tag{75}$$

which is identical to the particular solution found in the previous section.

Other than at $s = -2$, the poles of the transformed stresses are simple and the inversion gives the azimuthal stress as

$$\sigma_{\theta\theta}(\theta = 0) = \sum_{k=1}^{\infty} \left(\frac{-(s_k + 1)}{s_k}\right) \frac{1}{\left(\dfrac{\partial \Delta}{\partial s}\right)\bigg|_{s=s_k}} [Q_3 m' E' \alpha' \overline{T}'|_{s=s_k} + Q_4 k m'' E'' \alpha'' \overline{T}''|_{s=s_k}] r^{-(s_k+2)} \tag{76}$$

This gives the solution for the azimuthal stresses in bonded quarter planes as an infinite sum. The solution for the other stresses and displacements can be obtained in a similar manner.

To test the usefulness of the collocation technique, the material properties chosen for comparison of the two collocation methods earlier in this section were used to solve the half-space problem. The convergence of the series obtained from the Mellin transform inversion is demonstrated in Fig. 9, which plots the azimuthal interface stress on the symmetry line of the rectangle (at $r = l$) for increasing number of terms

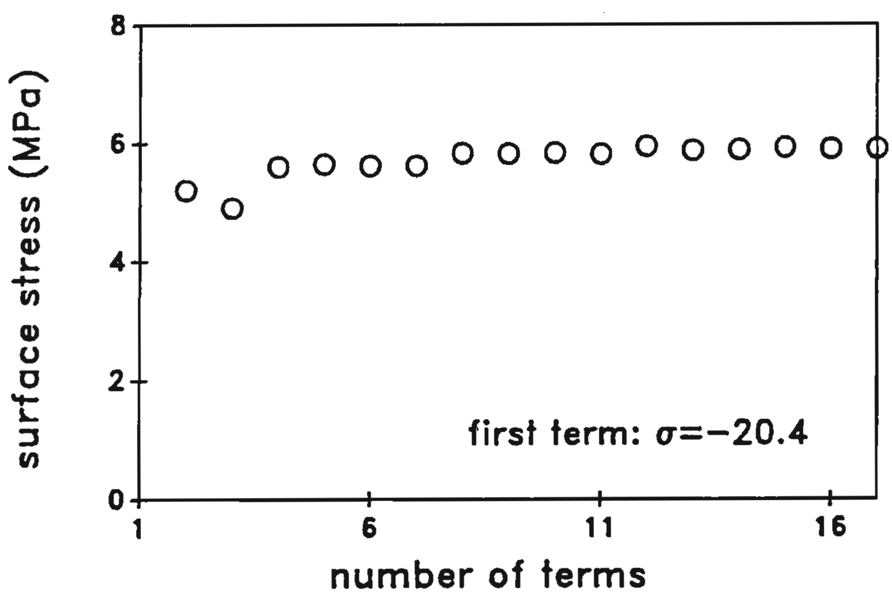

Fig. 9 Convergence of stresses at a given distance along the interface, as obtained by varying the number of terms obtained from the Mellin inversion.

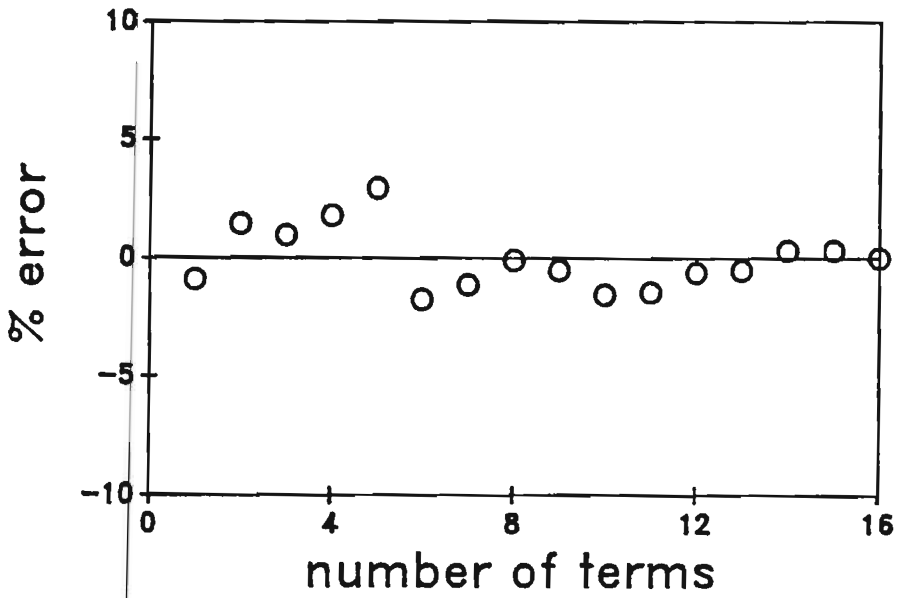

Fig. 10 Error in the boundary-layer stress intensity for collocation solution as compared to half-space solution.

in the series. This figure shows that the boundary stresses require only about a dozen terms in the series for accurate representation.

The rectangle extricated from the half-space model was analyzed by the collocation technique for comparison. The half-space solution is computed using 16 terms from the Mellin inversion, and the number of terms in the collocation solution is varied to test its convergence. The rectangle to be analyzed features a uniform temperature change and boundary conditions calculated from the half-space solution. The convergence of the first coefficient of the series with an increasing number of terms in the series is shown in Fig. 10, which shows the percent error in the collocation solution as compared to the known solution. This figure shows that the error is less than 1% when more than 12 terms are used. The peak errors in the surface stresses, calculated by using nine terms in the series, are roughly 25% of the particular solution, indicating that the first term in the series can be calculated with substantially greater accuracy than the surface stresses. Hence, it appears that the least squares collocation method yields accurate, reliable results for the asymptotic stresses near the edge of the interface.

CONCLUSIONS

The asymptotic behavior of singular thermal stress fields in finite bodies can be studied with the use of eigenfunction expansions. This technique provides acceptable results for the leading term in the expansion, even using relatively few terms in the series. The method, however, does not yield sufficiently accurate results for the far-

field stresses, becau
values and because
generated by the coll
least squares colloca
viding much faster ar
is much more reliab
like composition an
twice as many eigen

REFERENCES

1. Y. Weitsmann, Stre
terials, vol. 11, pp.
2. D. Chen, S. Cheng,
vol. 5, pp. 67–84,
3. H. E. Williams, As
Adhesive Layer, *J.*
4. M. L. Williams, Or
24, pp. 109–114, 1
5. D. B. Bogy, Edge-
J. Appl. Mech., vo
6. D. B. Bogy, On th
J. Solids Structures
7. S. S. Wang and I. C
Solutions and Basic
8. J. Fadle, Die Selbs
vol. 11, pp. 125–1
9. N. R. Bauld, Jr., a
for Calculating Fre
1985.
10. J. D. Whitcomb an
Stresses in Compo
11. N. J. Pagano and S
vol. 19, pp. 207–
12. W. H. Press, B. P
Cambridge Univer

field stresses, because of inaccuracies associated with determination of the eigenvalues and because of errors associated with solution of the ill-conditioned system generated by the collocation procedures. For determining the series coefficients, the least squares collocation method is superior to the point collocation method, providing much faster and more accurate convergence. Finally, this expansion technique is much more reliable when used for the analysis of singularities in composites of like composition and differing orientaton because, below a given value, there are twice as many eigenvalues and half of these are known analytically.

REFERENCES

1. Y. Weitsmann, Stresses in Adhesive Joints Due to Moisture and Temperature, *J. Composite Materials*, vol. 11, pp. 378–394, 1977.
2. D. Chen, S. Cheng, and T. Gerhardt, Thermal Stresses in Laminated Beams, *J. Therm. Stresses*, vol. 5, pp. 67–84, 1982.
3. H. E. Williams, Asymptotic Analysis of the Thermal Stresses in a Two-Layer Composite with an Adhesive Layer, *J. Therm. Stresses*, vol. 8, pp. 183–203, 1985.
4. M. L. Williams, On the Stress Distribution at the base of a Stationary Crack, *J. Appl. Mech.*, vol. 24, pp. 109–114, 1957.
5. D. B. Bogy, Edge-Bonded Dissimilar Orthogonal Elstic Wedges Under Normal and Shear Loading, *J. Appl. Mech.*, vol. 35, pp. 460–466, 1966.
6. D. B. Bogy, On the Problem of Edge-Bonded Elastic Quarter-Planes Loaded at the Boundary, *Int. J. Solids Structures*, vol. 6, pp. 1287–313, 1970.
7. S. S. Wang and I. Choi, Boundary-Layer Effects in Composite Laminates: Part 2—Free-Edge Stress Solutions and Basic Characteristics, *J. Appl. Mech.*, vol. 49, p. 549, 1982.
8. J. Fadle, Die Selbstspannungs-Eigenwertfunktionen der quadratischen Scheibe, *Ingenieur-Archiv*, vol. 11, pp. 125–149, 1941.
9. N. R. Bauld, Jr., and J. G. Goree, Comparison of Finite-Difference and Finite-Element Methods for Calculating Free Edge Stresses in Composites, *Comput. and Structures*, vol. 20, pp. 897–914, 1985.
10. J. D. Whitcomb and I. S. Raju, Reliability of the Finite Element Method for Calculating Free Edge Stresses in Composite Laminates, *Comput. and Structures*, vol. 15, pp. 23–37, 1982.
11. N. J. Pagano and S. R. Soni, Global-Local Laminate Variational Model, *Int. J. Solids Structures*, vol. 19, pp. 207–228, 1983.
12. W. H. Press, B. P. Flannery, S. A. Teukolsky, and W. T. Vetterling, *Numerical Recipes*, p. 54, Cambridge University Press, Cambridge, 1986.

Received October 27, 1989